Pigment–Pigment and Pigment–Protein Interactions in Recombinant Water-Soluble Chlorophyll Proteins (WSCP) from Cauliflower

ARTICLE *in* THE JOURNAL OF PHYSICAL CHEMISTRY B · DECEMBER 2007

Impact Factor: 3.3 · DOI: 10.1021/jp0723968 · Source: PubMed

Pigment−Pigment and Pigment−Protein Interactions in Recombinant Water-Soluble Chlorophyll Proteins (WSCP) from Cauliflower

C. Theiss,[†] I. Trostmann,[‡] S. Andree,[†] F. J. Schmitt,[†] T. Renger,[§] H. J. Eichler,[†] H. Paulsen,[‡] and G. Renger*,[||]

Institute of Optics, Technical University Berlin, Berlin, Germany, Institute of General Botany, Johannes Gutenberg University, Mainz, Germany, Institute of Chemistry, Free University of Berlin, Berlin, Germany, and Max Volmer Laboratory for Biophysical Chemistry, Technical University Berlin, Berlin, Germany

Received: March 27, 2007; In Final Form: August 31, 2007

Plants contain water-soluble chlorophyll-binding proteins (WSCPs) that function neither as antennas nor as components of light-induced electron transfer of photosynthesis but are likely constituents of regulatory protective pathways in particular under stress conditions. This study presents results on the spectroscopic properties of recombinant WSCP from cauliflower reconstituted with chlorophyll *b* (Chl *b*) alone or with mixtures of Chl *a* and Chl *b*. Two types of experiments were performed: (a) measurements of stationary absorption spectra at 77 and 298 K and CD spectra at 298 K and (b) monitoring of laser flash-induced transient absorption changes with a resolution of 200 fs in the time domain of up to 100 ps. On the basis of a theoretical analysis outlined by Renger et al. (*J. Phys. Chem. B* **2007**, *111*, 10487) the data obtained in part (a) are interpreted within a model where tetrameric WSCP binds predominantly two Chl molecules in the form of an excitonically coupled "open sandwich" dimer with a tilt angle of about 30° between the chlorin planes. The time-resolved measurements on Chl *a*/Chl *b* heterodimers are described by two exponential kinetics with time constants of 400 fs and 7 ps. These kinetics are assumed to reflect a heterogeneous population of WSCPs with Chl dimers either in excitonic coupled "open sandwich" or weakly coupled geometric arrays. The 400 fs component is assigned to excited-state relaxations from the upper to the lower excitonic level of the strongly coupled "open sandwich" dimer, while the 7−8 ps component probably indicates excitation energy transfer from ^{1}Chl *b** to Chl *a* in a dimer array with weak coupling due to significantly longer mutual distances between the chlorin rings.

Introduction

The key steps in the transformation of solar radiation into Gibbs energy via the photosynthesis process take place in pigment−protein complexes referred to as reaction centers (RCs) in anoxygenic bacteria and photosystems I and II (PS I and PS II) in oxygen-evolving organisms. The RCs of the former type of organisms contain bacteriochlorophyll (BChl) molecules as photoactive pigments, while in the latter type of organisms chlorophylls (Chls) replace the BChls (for a review, see ref 1).

Electron ejection from the lowest excited singlet state of a special (B)Chl unit leads to formation of a cation−anion radical pair that is stabilized by subsequent electron-transfer reactions, thus providing the driving force for sequences of metabolic processes eventually leading to reduction of CO_2 to carbohydrates. Photosynthetic organisms are exposed to illumination conditions that vary in times (diurnal, seasonal changes) and depend on space, i.e., the nature of the biotope (e.g., different altitudes in a rainforest or water depths in oceans). Suitable adaptation mechanisms are required in order to cope with these demanding circumstances. This important goal has been achieved by the development of pigment−protein complexes that simultaneously fulfill two functions: (i) light harvesting at limiting photon flux densities through efficient funneling of electronically excited states formed by light absorption to the photoactive pigment of the RCs and photosystems and (ii) on the contrary, opening of dissipative channels for radiationless decay of superfluous populations of excited states formed at high light intensities to protect against deleterious effects (photoinhibition) and therefore need to be diminished.

The photosynthetic antenna complexes contain only three classes of chromophore ((bacterio) chlorophylls, phycobilins, and carotenoids) and belong mainly to seven major protein families (LH1, LH2, LH3, chlorosomes, the FMO protein, phycobilisomes, the LHC superfamily, and the peridinin Chl *a*-protein) (for a review, see ref 2). In these complexes the excitation energy transfer (EET) processes are determined by pigment−pigment and pigment−protein interactions (for reviews, see refs 3 and 4). Direct pigment−lipid interactions are rare, but lipids play an essential indirect role in formation of aggregates of pigment−protein complexes. An illustrative example is the requirement of phosphatidylglycerol (PG) and digalactosyldiacylglcerol (DGDG) for formation and structural integrity of LHC II trimers.[5−7] All Chl-binding proteins that are involved in the photosynthesis of higher plants are hydrophobic and integrated into the thylakoid membrane (for reviews, see refs 8 and 9).

In addition to these pigment−protein complexes constituting PS I and PS II with the antenna systems, higher plants contain

* To whom correspondence should be addressed.
[†] Institute of Optics, Technical University Berlin.
[‡] Johannes Gutenberg University.
[§] Free University of Berlin.
[||] Max Volmer Laboratory for Biophysical Chemistry, Technical University Berlin.

10.1021/jp0723968 CCC: $37.00
Published on Web 11/02/2007

another type of Chl-binding proteins. These complexes are hydrophilic water-soluble chlorophyll proteins (WSCPs) that were found in Brassicaceae, Polygonaceae, Chenopodiaceae, and Amaranthaceae families and appear in two classes which differ in the response of their absorption changes to illumination: Class I WSCPs exhibit a significant red shift upon illumination, while Class II WSCPs show no photoconversion (for a review, see ref. 10). The functional role of the WSCPs is not yet resolved and a matter of speculation. WSCPs are not found in thylakoids but may be—at least transiently—located in the endoplasmic reticulum.[11] Therefore, the WSCPs are most likely not another type of antenna, i.e., they are involved neither in the light harvesting nor in protective dissipation of excess population of excited states of the mature photosynthetic apparatus. One striking feature is the stimulation of WSCP formation under drought,[12] salt,[13] and heat[14] stress or after leaf detachment.[15] Therefore, it seems attractive to speculate that the complex might provide protection against degradative processes.

The WSCPs are characterized by two striking properties: (i) the high affinity for binding of chlorophylls and related compounds, accompanied by oligomerization (in most cases to tetramers), thus extracting Chls very efficiently from the thylakoid membrane,[11,16] and (ii) the presence of a Künitz-type motif in the sequence of all WSCPs.[10] The former property suggests a possible role as a Chl-binding and carrier protein. One hypothesis assumes that during senescence of leaves WSCP acts as a Chl carrier which transports the pigments to the inner envelope membrane[10] where the enzyme chlorophyllase initiates the degradation process.[17,18] As an alternative possibility, WSCP could act as a binding protein of Chl precursors in the biosynthesis pathway of Chl,[19] but in the case of binding of pigments without a phytyl chain (e.g., chlorophyllide) no oligomerization can occur.[16] It has been shown that a WSCP homolog from *Hordeum vulgare* (barley) can bind chlorophyllide and accumulates in the chloroplasts after exposure to light,[20] which led the authors to propose a role as a pigment carrier during light-induced chloroplast development. This result, coupled with the finding that WSCP is able to bind Chl derivatives,[16] indicates a possible function as a carrier of Chl precursors during Chl biogenesis. On the other hand, the presence of a Künitz-type motif is a structural characteristic for protease inhibitors, but so far no proteinase inhibitor function has been found for the WSCP type analyzed in this study but for other types of WSCP a pH dependent protease activity was reported.[44]

Another interesting feature is the lack of any carotenoid binding, i.e., WSCPs are the only Chl-binding proteins known so far that do not contain carotenoids.[16] This raises questions on the markedly diminished sensitized singlet-oxygen formation by Chl bound to WSCP compared to that in solution.[16] Several possible mechanisms have been discussed to explain this phenomenon, but so far an unambiguous answer is still lacking (this problem will be discussed in a forthcoming paper by Schmitt et al.).

Apart from the unresolved localization in plant cells and open questions regarding the functional role of WSCP, this Chl-binding protein appears to be a very interesting system. For three reasons it provides a most suitable sample material to study the properties of Chls bound to proteins: (i) it is the only type of natural Chl-binding protein known so far that completely lacks carotenoids (vide supra), (ii) the protein matrix of about 20 kDa[15] is comparable with the size of the LHC family but houses only one pigment at most in marked contrast to LHC II and related members of this family containing many pigments (for a review, see ref 22), and (iii) the DNA from cauliflower-WSCP can be expressed in *E. coli*, and the recombinant protein can be reconstituted with Chl molecules to tetramers that are very similar to native WSCP isolated from cauliflower.[11] Therefore, complexes of recombinant WSCP reconstituted with Chl are expected to offer a simple and well-defined sample material for thorough analysis of pigment−pigment and pigment−protein interactions and detailed studies on the excited-state dynamics. In a recent report[23] stationary absorption and magnetic circular dichroism (MCD) spectra were measured at 1.7 K on recombinant WSCP reconstituted with either Chl *a* or Chl *d*.

Evaluation of these data on the basis of an exciton model led to the proposal for the arrangement of Chl *a* and Chl *d* in the form of an open sandwich dimer.[23] The tilt angle of the chlorin planes of the Chl moieties was inferred to be about 60°. A detailed theoretical analysis based on the stationary absorption and CD spectra led to the conclusion that the angle is only 30°.[24] This result is in perfect agreement with the recently reported structure gathered from X-ray diffraction crystallography for a class IIB WSCP from *Lepidium virginicum*.[25] In these WSCPs the Chls were found to form an open sandwich dimer with an angle of 27°. WSCP samples provide a suitable material to analyze the excitonic structure of the open sandwich dimer and in particular the excited dynamics.

The present study addresses these problems by measurements of (i) stationary absorption spectra monitored at room temperature and 77 K and the CD spectrum at room temperature and (ii) laser flash-induced transient absorption spectra with a time resolution of 200 fs at room temperature on WSCP samples reconstituted either with Chl *b* only or with mixtures of Chl *a* and Chl *b*. The results obtained reveal that homo- and/or heterodimers of the pigments with strong excitonic coupling are formed, in line with the proposal of Chl *a* and Chl *d* homodimers.[23] The excited-state dynamics exhibit characteristic biphasic kinetics with time constants of 400 fs and 7−8 ps that are explained by exciton-state relaxation and excited-state energy-transfer processes, respectively.

Materials and Methods

Sample Material. *Protein.* Recombinant WSCP from cauliflower (*Brassica oleracea* var. Botrys) with an N-terminal hexahistidyl (His) tag was expressed as previously described[16] with some modifications. Following induction of WSCP expression with IPTG, the growth temperature was reduced to 28 °C and protein expression was continued under these conditions over night. After cell lysis and centrifugation, the supernatant containing soluble WSCP was stored in aliquots at −20 °C to be used for sample preparation.

Pigment. Total pigment extract was obtained from pea plants as previously described.[26] Purified Chl *b* was prepared as described in Hobe et al.[27] Aliquots of pigments were dried and stored at −20 °C in inert (nitrogen) atmosphere.

Reconstitution of Chl-WSCP. Reconstitution and purification of soluble WSCP was performed simultaneously by binding the protein to a Chelating Sepharose Fast Flow (Amersham Biosciences) column charged with Ni^{2+} ions and equilibrated with 50 mM Na phosphate pH 7.8. The sample was filtered before loading on the column at 2 mg of WSCP per milliliter of column material. After removal of contaminating bacterial proteins by washing with 10 column volumes of 50 mM Na phosphate pH 7.8 and following equilibration of the column with 5 column volumes of 50 mM Na phosphate pH 7.8/12.5% sucrose/1% octyl-β-D-glucopyranosid (NaP-OG-buffer), the

protein was incubated with a 5-fold molar excess of Chl (total pigment extract or purified Chl *b*), presolubilized in 100% ethanol at 10 mg/mL, and then diluted 20-fold with NaP-OG-buffer. The pigment solution was thoroughly dispersed with the column material and then incubated for 1−2 h at room temperature under protection from light. To obtain WSCP with a Chl/protein ratio of 0.09, Chl and protein were mixed at a molar ratio of 0.25:1, and the procedure was modified in that the column material with bound WSCP was vigorously vortexed during addition of pigment in order to ensure that the Chl was immediately evenly distributed. Unbound Chl was removed by a thorough wash with 30 column volumes of NaP-OG-buffer. After detergent removal by washing with 10 column volumes of 50 mM Na phosphate pH 7.8, the purified and reconstituted pigmented protein was eluted from the Ni^{2+} column with 20 mM Na phosphate pH 7.8/300 mM imidazole/2 mM β-mercaptoethanol and subsequently concentrated in Centricon devices (30 kDa MW cutoff, Millipore), so that the sample had an OD at 673 nm of at least 1 at a path length of 2 mm. For measurement of laser flash-induced transient absorption spectra, samples with an OD_{673} exceeding this value were diluted accordingly with elution buffer. Determination of the pigment composition and pigment to protein ratio was performed as described in Schmidt et al.[16] It should be noted that the Chl *a/b* ratios mentioned in this paper refer to the ratio of bound Chl *a* and *b*. These ratios were randomly obtained during the respective reconstitutions and depended on the solubility of the chlorophylls in the pigment solution. Using the above-mentioned reconstitution method, no evidence was found that recombinant cauliflower-WSCP exhibits preference for either Chl *a* or *b*, as determined in a titration experiment with varying Chl *a/b* ratios (data not shown).

Measurements. *(a) Stationary Absorption and CD Spectra.* Ground-state absorption spectra were recorded with a UV−vis scanning spectrophotometer (UV-2101PC, Shimadzu) in a range from 350 to 750 nm with medium scan speed and a bandwidth of 1 nm. Absorption spectra (77 K) were measured in the region from 600 to 750 nm, and data from nine consecutive measurements of each sample were averaged. CD spectra were measured at RT with a Jasco J-810 spectropolarimeter using a quartz cuvette with a path length of 2 mm, scan speed of 100 nm/min, bandwith of 4 nm, data pitch of 0.5 nm, and response time of 2 s.

(b) Time-Resolved Transient Absorption Spectra. Laser flash-induced transient absorption spectra were recorded on home-built equipment with a time resolution of about 200 fs. A diode-pumped frequency-doubled Nd:YVO-laser (Millenia, Spectra Physics) was used for pumping a Ti:Sa-Oscillator (Tsunami, Spectra Physics) which produces pulses of 70 fs duration at 800 nm. The pulse energy is amplified from some nanojoules to one millijoule using a regenerative amplifier system (Spitfire, Spectra Physics). The output of the amplifier system is used for pumping a white light seeded, two-stage collinear optical parametric amplifier (OPA 800F, Spectra Physics) to generate tunable excitation pulses in the whole visible spectral range. Typically, pulses with a spectral width of about 12 nm at a repetition rate of 1 kHz can be generated. The linear chirp of the 160 fs output pulses of the OPA is compressed to a pulse duration up to 70 fs using a home-built grating compressor. During the experiments the pulse duration was continuously controlled with a home-built frequency-resolved gating system (FROG) that allows online characterization of the red and near-infrared femtosecond laser pulses.[28] After passing a variable translation stage (minimum step 0.5 μm) the pulses were directed to the WSCP sample in the pump−probe apparatus where they acted as pump pulses. Pump energies of 140−200 nJ have been used for sample excitation. Assuming typical Chl concentrations of 50 μg/mL in these measurements, a laser spot size of about 200 μm, and an optical pathway of 2 mm the single hit probability of each Chl molecule in the illuminated sample volume is less than 5%. Accordingly, multiple excitations of Chls in a single WSCP tetramer are negligible. A fraction with 60 μJ of the residual laser pulses at 800 nm is focused on a rotating cuvette of 5 mm optical pathway containing D_2O, thus generating bright white light continuum pulses ranging from 500 nm to the infrared that are used for probing the absorption change in the sample. The dispersed white light can be compressed down to about 180 fs using another grating compressor. In addition, the intense frequency components around 800 nm and other infrared contributions are suppressed when trespassing the compressor.

The white light beam overlaps with the pump beam at an angle of 5° in the center of a fused silica cuvette with 2 mm optical path length. The polarization difference between the beams is set to the magic angle of around 54.7° to minimize polarization effects during measurement. A small fraction of the white light is split off in front of the sample and used as reference beam.

The transmitted probe beam and reference beam are collected with a CCD-Kamera (Princeton Instruments CCD576-TE) with 16-bit dynamic range mounted on a polychromator (Mc Pherson). This allows the simultaneous detection of absorption changes in a 190 nm section with a spectral resolution of around 0.5 nm. Data of 30 000 laser shots per time delay step between pump and probe pulse in a time window 0−100 ps were accumulated, and transient absorption changes were calculated with a resolution of $\Delta A \approx 5 \times 10^{-4}$.

All samples were stirred during the measurements using a magnetic stir bar. The cuvettes were flushed with nitrogen after filling to decrease possible oxygen-induced effects in the samples. No sample degradation during the measurements was observed, but influences on the samples due to oxygen cannot be excluded completely.

Results

Ground-State Absorption. Native WSCP from cauliflower exhibits a Chl *a/b* ratio of about 6:1.[29] The recombinant WSCP can be successfully reconstituted with a variety of pigments at different pigment ratios.[13] In the present study mainly three different types of reconstituted WSCP have been investigated: (i) samples with Chl *a/b* ratios of 4.2:1, (ii) samples with Chl *a/b* ratios of 2.6:1, and (iii) samples containing exclusively Chl *b*.

Figure 1 shows the absorption spectra monitored at room temperature on both sample types containing Chl *a*/Chl *b* at two different ratios. These spectra exhibit a similar shape originating basically from the absorption profiles of the chlorophylls. Closer inspection reveals characteristic differences in the blue and red region that are most pronounced at 460 nm, i.e., in the Soret band of Chl *b*. Therefore, these differences are due to the Chl *a/b* ratios of 4.2:1 and 2.6:1.

In the red spectral range the absorption of both samples is characterized by a peak with a maximum at 673 nm and a clearly resolved shoulder at around 660 nm in the sample with the higher Chl *b* content. Furthermore, a smaller peak emerges at 628 nm, which can be assigned to the vibrationally coupled $Q_y(1,0)$ transition, while the shoulder at around 580 nm reflects the $Q_x(0,0)$ transition.[30] The more pronounced $Q_y(1,0)$ band in

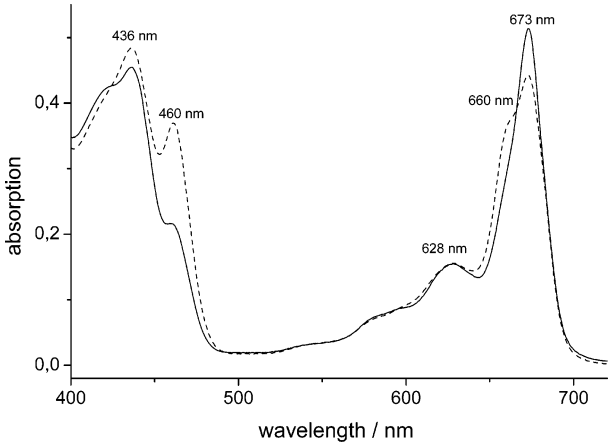

Figure 1. Ground-state absorption spectra of WSCP with Chl *a*/*b* ratio = 4.2:1 (continuous line) and Chl *a*/*b* = 2.6:1 (dotted line) at room temperature.

comparison to diluted Chl solutions is assumed to be caused by specific pigment−protein interaction. A fit analysis with Gaussians of the red band of the two samples deconvoluted the absorption profiles of the Q_y band into five major components with peak positions at 653, 662, 671, 677, and 685 nm, as shown in Figure 2. The peak wavelengths of these Gaussian bands are in almost perfect agreement with the results obtained by Satoh et al.[11] for native and recombinant MBP-(maltose-binding protein) WSCP (peak positions at 652, 663, 671, 677, and 685 nm). In this report only the component at 653 nm has been assigned to Chl *b*, while the other bands (including the 663 nm band) are ascribed to Chl *a*. This proposal, however, is hardly reconcilable with the strikingly larger contribution of the 662 nm band in the experimental spectrum (and the deconvolution into Gaussians) of the sample with the higher Chl *b* content. This marked difference rather suggests that the 662 nm band is preferentially originating from Chl *b*. This conclusion would imply that—to the best of our knowledge—the interaction of the pigment with its environment in the WSCP complex, including the possibility of excitonic coupling with another Chl molecule, gives rise to the "red most" absorbing Chl *b* molecule in a pigment−protein complex. The Gaussian bands with peak positions at 671, 677, and 685 nm are assigned to bands with Chl *a* character. Although there is only one binding position per subunit, the Chls bound in tetramers show characteristic differences. Accordingly these spectral features raise questions on the mode of Chl binding in WSCP.

For further characterization of the properties of Chl *b* binding, absorption and CD spectra were measured on a WSCP sample which was reconstituted solely with Chl *b*. Figure 3 shows the spectra monitored at room temperature (left) and the absorption spectrum together with its fourth derivative at 77 K (right). The absorption at room temperature exhibits a maximum at 657 nm in the red region of the spectrum. This position is shifted to the blue by about 5 nm as compared with the Gaussian band at 662 nm gathered from the deconvolution of the spectra of Figure 2 for samples containing Chl *a* and Chl *b*. At 77 K the maximum slightly shifts to 656 nm and a clearly discernible shoulder emerges at the long wavelength side. Analysis of the fourth derivative of the spectrum results in two subbands at 655.6 and 664.0 nm. This feature of a band splitting is not specific for the Chl *b*-binding WSCP. Similar spectral characteristics were found by Hughes et al.[23] for the absorption spectra of recombinant WSCPs that are reconstituted either with Chl *a* or with Chl *d*. The band splitting is reminiscent of the properties of an excitonically coupled homodimer. Accordingly Hughes et al. interpreted their findings by the assumption of two strongly excitonically coupled pigments in an "open sandwich" geometry.[23] An analogous excitonically coupled homodimer of two Chl *b* molecules is most likely to be formed also in the pure Chl *b*−WSCP. This idea is highly supported by the circular dichroism (CD) spectrum of the Chl *b*−WSCP measured at room temperature (see Figure 3a, dashed line) that exhibits two signals of opposite signs at 655 and 667 nm. CD bands with opposite sign and areas of roughly the same size are characteristic of a strongly coupled homodimer. Gaussian deconvolution of the absorption profile of the Q_y band led to the same subband positions when analyzing the fourth derivative, but an additional lower band centered at 649 nm was necessary to describe the blue wing of the absorption profile (data not shown). Possibly the 653 nm band in the Chl *a*/Chl *b*-containing WSCP (Figure 2) corresponds to a small fraction of Chl *b* homodimers that cannot be resolved sufficiently in this analysis. On the basis of our finding that there is no preference to the binding of either Chl *a* or Chl *b*, the fraction of Chl *b* homodimers is estimated to be about 3.7% and 7.7% for samples with Chl *a*:Chl *b* = 4.2:1 and Chl *a*:Chl *b* = 2.6:1, respectively.

In order to obtain more information on the possible geometry of the putative excitonically coupled dimer, simulations of the ground-state absorption and CD spectra of the Chl *b*−WSCP were performed on the basis of the "open sandwich" model of an excitonically coupled dimer proposed by Hughes et al.[23] The details of our calculations are described in ref 24. The results obtained led to a similar center-to-center distance of 7.4 Å between the two coupled Chl *b*−pigments as reported for the Chl *a* homodimer. However, the angle of around 36° obtained for a best fit is significantly smaller than the value of 60° gathered by Hughes et al.[23] from their analysis of the Chl *a* homodimer in the WSCPs.

The results reported thus far strongly support the existence of homodimers in recombinant WSCP complexes reconstituted exclusively with either Chl *a*[23] or Chl *b* (this study). Therefore, the question arises whether the excitonically coupled dimer is the only pigment-binding motif in cauliflower WSCP. It is well known that WSCPs tend to oligomerize mainly to tetramers when the apoprotein is reconstituted with Chls. An average value of 0.5 Chls bound per WSCP (2 Chls per tetramer) was found in all sample preparations analyzed in this study, where the Chl concentration in the reconstitution assay was saturating. This statistical value of the ensemble could be the result of different numbers and arrangements of the pigments within the individual tetrameric WSCP complexes (multistate ensemble) or reflect the highly preferred formation of pigment dimers only ("quasi single occupation" state ensemble). In order to address this question we compared the absorption spectra of two different sample preparations which greatly differed in their overall Chl/protein stoichiometry, i.e., preparations with ratios of 0.57 and 0.09. In the case of a multistate ensemble, the absorption profiles should strongly depend on the total Chl/protein ratio, i.e., WSCP complexes containing a single Chl per molecule should be the dominant form in the samples with 0.09 Chl/protein. Figure 4 shows a plot of absorption spectra that were measured at 77 K and normalized to the peak position at 673 nm. At first glance the spectral profiles of the two sample types exhibit a striking similarity. The largest difference is observed at around 657 nm, which can be accounted for by the different Chl *a*/*b* ratios of the two preparations. Closer inspection also reveals slight differences in the region of the Chl *a* absorption; in particular, the shoulder at the "red edge" is of somewhat smaller amplitude in the sample with the very low total Chl content. Two

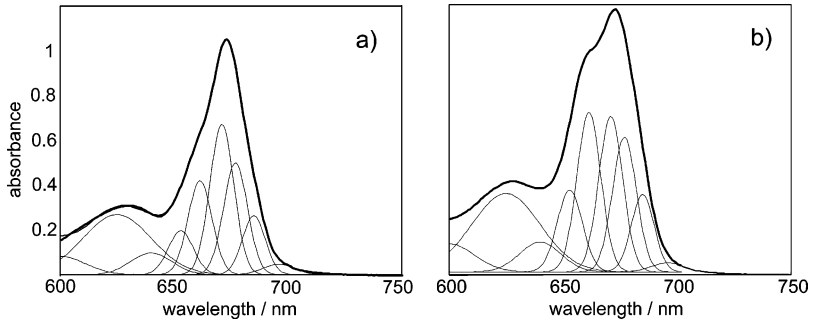

Figure 2. Gaussian band deconvolution of the ground-state absorption spectra of WSCP with Chl *a*/*b* ratio = 4.2:1 (a) and Chl *a*/*b* = 2.6:1 (b) at room temperature.

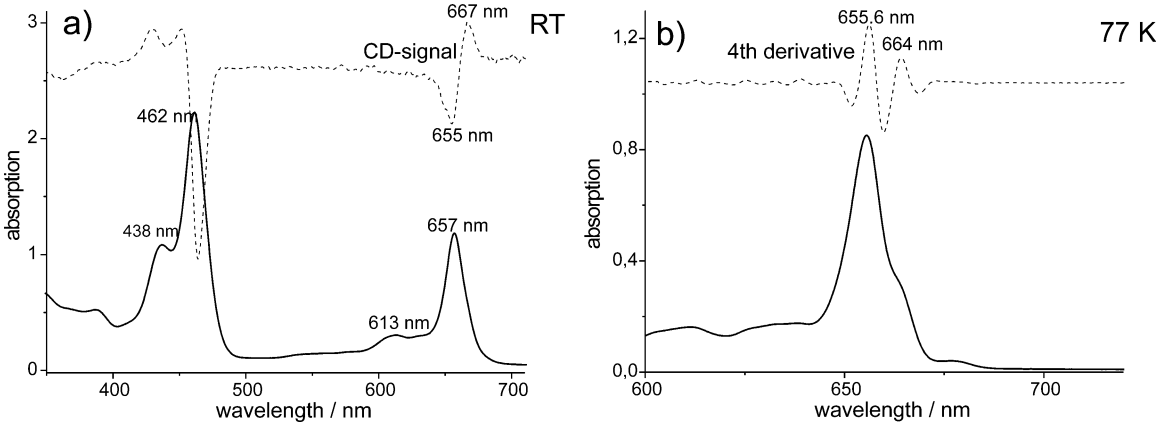

Figure 3. Chl *b*-WSCP: ground-state absorption (straight line) and CD spectra (dashed line) at room temperature (a), and ground-state absorption spectrum at 77 K (continuous line) and its fourth derivative (dashed line) (b).

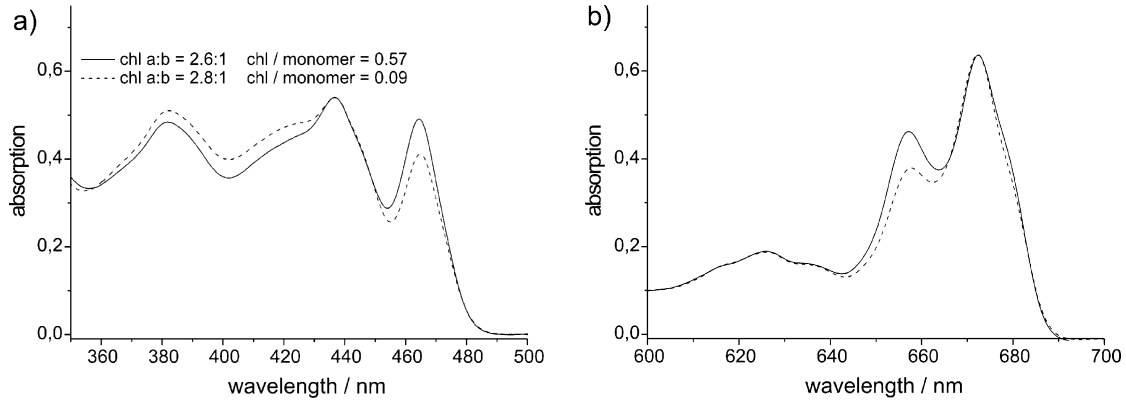

Figure 4. Normalized absorption spectra at 77 K of recombinant WSCP samples reconstituted with different total amounts of chlorophylls at similar Chl *a*/*b* ratios (a) in the Soret band and (b) in the Q-band.

conclusions can be gathered from these findings: (i) the ratio of 2 Chls per tetramer is not only an average value but each recombinant WSCP apoprotein from cauliflower binds two pigments when recombined with Chls under formation of tetramers and the population probability of other forms (tetramers containing one, three, or four Chls) is rather small or even zero and (ii) the less pronounced shoulder in WSCP samples reconstituted at very low Chl concentrations suggests that these samples contain a smaller total fraction of excitonically coupled Chl *a*/Chl *b* pairs due to either a minor fraction of tetrameric complexes with only one Chl or formation of tetramers with two Chls that are not strongly excitonically coupled.

Laser Flash-Induced Transient Absorption Changes. Analysis of the ground-state absorption and CD spectra revealed that Chl *b* forms homodimers with strong excitonic coupling in recombinant WSCP reconstituted with that pigment only. When taking into consideration that the same pattern is found in recombinant WSCPs reconstituted with either Chl *a* or Chl *d* alone[23] it can be expected that in samples containing both Chl *a* and Chl *b* these pigments very likely bind as heterodimers with strong excitonic coupling. In addition, Chl *a*/Chl *a* homodimers are formed due the excess of Chl *a*. These homodimers are characterized by a much smaller energy gap between the upper and lower exciton level. Therefore, the Chl *a*/Chl *b* heterodimers provide a very suitable material for studying the dynamics of electronically excited states. In these heterodimers the wave function of the upper exciton band is dominated by the contribution of Chl *b*.

For this reason the samples were excited with pulses of peak wavelengths of 650 (data not shown) and 460 nm, which are predominantly absorbed by the Q_y and Soret band, respectively, of Chl *b*. Changes of the absorption spectra in the range from

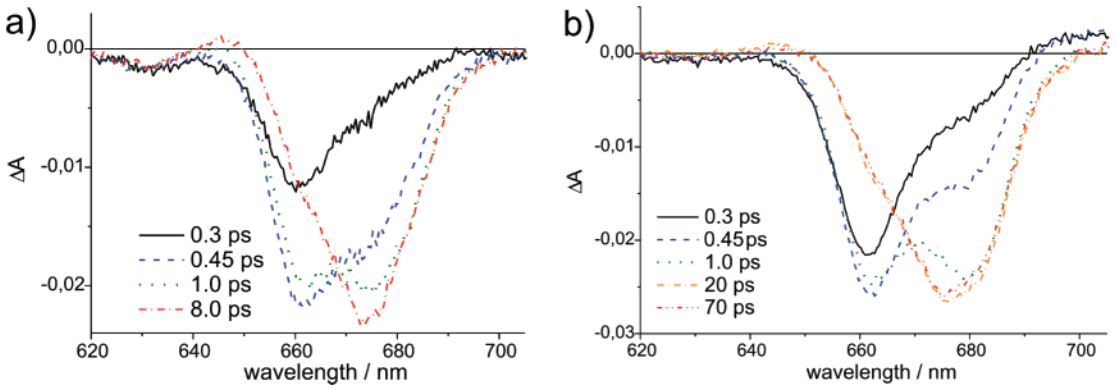

Figure 5. Transient absorption difference spectra induced by 460 nm excitation ($\tau \approx 100$ fs, $E = 140$ nJ) in Chl *a* and Chl *b* containing WSCP [(a) Chl *a*/*b* = 4.2:1, (b) Chl *a*/*b* = 2.6:1] at different delay times between pump and probe pulses.

630 to 705 nm were monitored at various delay times between the pump and probe pulses in a time window of 0.2−70 ps.

Measurements performed in the Q_y transition ($\lambda_{ex} = 650$ nm) are complicated by simultaneous excitation of exciton bands originating from both Chl *a* and Chl *b* due to the small energetic gap between the transitions in these two pigment molecules. The spectral difference between Chl *a* and Chl *b* is markedly larger in the Soret band. Therefore, experiments were performed with pump pulses at a wavelength of 460 nm where the Soret band of Chl *b* exhibits its peak position while the absorption of Chl *a* is much smaller (see Figure 1). Under these excitation conditions the probability of direct excitation at 460 nm of Chl *a*/Chl *a* homodimers is expected to be small, despite the rather broad spectral width (fwhm = 12 nm) of the laser pulses.

Figure 5 shows difference spectra that are monitored at different delay times between the pump and the probe pulse. After short delay times ($t < 0.4$ ps) the bleaching exhibits a pronounced band with a peak at around 660 nm in the Chl *b* spectral region that is assigned to the population of the upper exciton band of the heterodimer. At longer delay times the extent of the Chl *b* bleaching decreases concomitant with a progressing increase of the bleaching in the Chl *a* region, approaching a maximum value at $t = 0.9$ ps and a peak maximum at 679 nm. In the time domain of $t > 1$ ps the absorption maxima shift back to shorter wavelengths and reaches a virtually constant peak position at 675 nm after a delay time of about 10 ps, but shoulders of the bleaching at around 660 and 680 nm still remain.

This feature is indicative of a fast excitation energy transfer from the upper to the lower exciton bands of the dimers, as discussed in detail further below. At longer delay times up to the limit of the detectable time window of 70 ps no further changes in the bleaching are observed for both Chl *a* and Chl *b*. The decay of the excited singlet states of Chl *a* and Chl *b* in WSCP was shown to be in the range of a few nanoseconds (Schmitt et al., manuscript in preparation) and cannot be detected by the measurements at the time window of 70 ps.

The transient band shift from 679 to 675 nm cannot be explained by relaxation of vibrational modes of the protein excited by the laser pulses because in this case a band shift of opposite direction, (i.e., to lower energies) would arise. It seems reasonable to assume that this feature reflects the existence of weakly coupled dimers (vide infra). The excitation at 460 nm populates higher excited singlet states followed by relaxation into S_1. Therefore, the kinetics of the energy transfer could be effected by the time course of the internal conversion. However, the latter is expected to be fast enough to be not rate limiting, and consequently, the present setup of excitation at 460 nm gives rise to a significant population of the high-energy exciton state of the heterodimers whereas excitation at 650 nm does not.

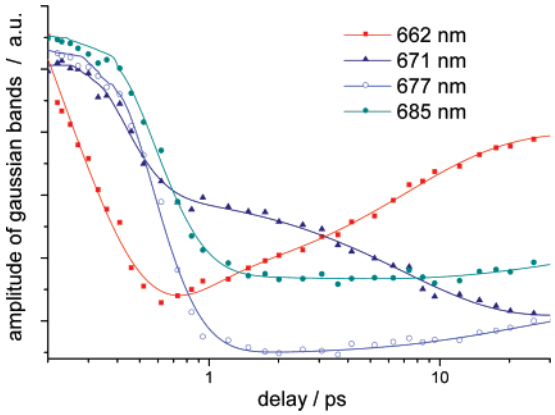

Figure 6. Amplitudes of Gaussian bands gathered from deconvolution of the transient absorption spectra in Figure 5b.

The time course of transient absorption spectra induced by 460 nm pump pulses was analyzed at different wavelengths in the Q_y band based on the same Gaussian band deconvolution procedure that was used for the steady-state absorption spectra with peak maxima at 662, 671, 677, and 685 nm (see Figure 2). Figure 6 shows the time course of the amplitudes of the four major Gaussians with peaks at 662, 671, 677, and 685 nm (see Figure 2).

The decay of the bleaching at 662 nm Gaussian band (dominated by the Chl *b* contribution) as a function of the delay time between pump and probe pulse can be satisfactorily described by a biphasic kinetic with time constants of 400 fs and 7−8 ps after temporal deconvolution of the data with an instrumental response function of 200 fs. The other three Gaussians with peaks at 671, 677, and 685 nm are assigned to bands of Chl *a* character. All three bands exhibit biphasic rise kinetics with time constants (400 fs, 7−8 ps) that correspond with the values obtained for the decay of the 662 nm band. Marked differences exist in the relative contribution of the kinetics to the overall time course. The rise of the two "red most" bands at 677 and 685 nm occurs almost exclusively with the 400 fs kinetics, while the band at 671 nm is largely dominated by the 7−8 ps kinetics with a rather small contribution of the 400 fs component. Before we discuss the origin of the slow component we analyze the fast one.

Two alternative possibilities have to be considered for the origin of the 400 fs kinetics: (i) excitation energy transfer from ^{1}Chl *b** to "red" Chl *a* molecules or (ii) relaxation between the upper and lower excitonic state of a strongly coupled pigment heterodimer. In the case of ii the existence of a nondecaying

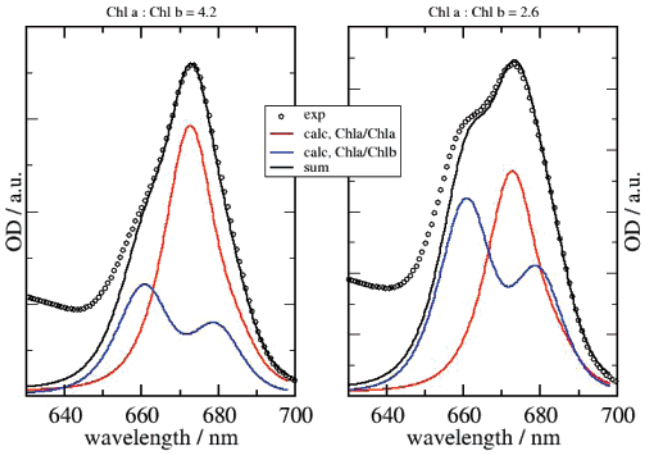

Figure 7. Linear absorption spectra of WSCP reconstituted at different Chl *a*:Chl *b* ratios. The experimental data are the same as in Figure 2. The calculations (solid lines) are based on the exciton model.[24] The spectra were modeled by taking into account formation of Chl *a*/Chl *b* heterodimers (blue lines) and Chl *a*/Chl *a* homodimers (red lines) at different ratios.

fraction of the bleaching in the Chl *b* region would be a signature of a partly delocalized exciton state. In the case of i one would have to assume that there is a small fraction of WSCP complexes with a Chl *b* dimer in order to account for the remaining bleaching at 662 nm. However, the ground state bleaching of the upper exciton state of a Chl *b* homodimer is expected to be observed at a somewhat shorter wavelength (657 nm). Native WSCP from cauliflower binds Chl *a* and Chl *b* in a ratio of about 6:1.[29] If the recombinant apoprotein affinity would exhibit a similar preference for Chl *a* compared to Chl *b* (see Materials and Methods), from a statistical point of view the percentage of WSCP-tetramers containing two Chl *b* pigments is expected to be significantly smaller than the ratios of 3.7% and 7.7% obtained when ignoring selectivity in all binding (vide supra). This idea is supported by fluorescence measurements (Schmitt et al., manuscript in preparation).

Case ii will be considered in the following by analyzing the pump−probe spectra in the framework of an exciton model developed recently.[24] For this purpose, the heterodimer absorption spectra in Figure 2 are compared in Figure 7 with our exciton calculations[24] that are based on an open sandwich model of Chl *a*/Chl *a* homodimers (red lines) and Chl *a*/Chl *b* heterodimers (blue lines) with strong excitonic coupling. The spectra of the homo- and heterodimers were added taking into account the different Chl *a*:Chl *b* ratios in the two experiments. The data of Figure 7 reveal that the heterodimer is characterized by exciton states at around 660 and 680 nm, whereas the oscillator strength of the homodimer is concentrated in an exciton transition at about 675 nm.

The deviations at the blue side between calculated and experimental spectra are due to neglecting the excitation of a higher excited electronic state and/or intramolecular vibrational states in the underlying exciton model.[24] For a given ratio *x* of Chl *a*:Chl *b*, the ratio of homo- to heterodimers in the sample is $(x - 1)/2$ if the fraction of Chl *b*:Chl *b* homodimers is negligibly small. Hence, we know that there are twice as many heterodimers present at the lower Chl *a*:Chl *b* ratio of $x = 2.6$ as compared to the sample with $x = 4.2$. However, the ratio of homo- to heterodimers that are excited at 460 nm in the pump−probe experiment is not exactly known. A higher excitation probability is expected for the heterodimers compared with the Chl *a* homodimers since Figure 1 demonstrates that the strongest drop is observed for the 460 nm band when the Chl *b* content

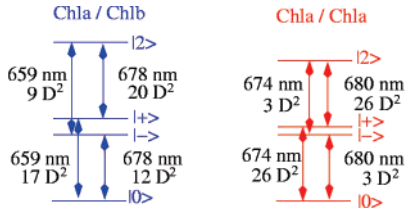

Figure 8. Dipole strengths and transition wavelengths between the ground state $|0\rangle$ and the one exciton states $|+\rangle$ and $|-\rangle$ and between the latter and the two exciton states $|2\rangle$ for the hetero- (left) and homo- (right) dimer. The exciton states are calculated on the basis of the exciton model proposed in ref 24.

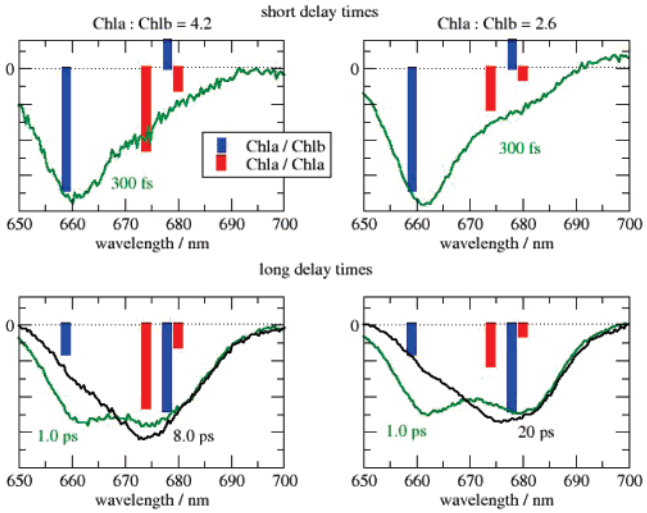

Figure 9. Comparison of exciton stick spectra and experimental pump−probe data from Figure 5. For the stick spectra it was assumed that at short delay times the high-energy exciton state of the heterodimers and the low-energy state of the homodimers are populated, whereas at long delay times both dimers are populated in their low-energy exciton state.

is decreased. Closer inspection of the pump−probe spectra measured at two different values of *x* in Figure 5 reveals three differences: (i) there is a small but significant positive signal at short delay times for $x = 2.6$ (b), (ii) the ratio of bleaching at 660 and 680 nm at 0.3 ps delay is larger for $x = 2.6$ than for $x = 4.2$, and (iii) the position of the long wavelengths bleaching at 1 ps is at 680 nm for $x = 2.6$ and at 675 nm for $x = 4.2$ (compare a and b).

These findings can be qualitatively explained by first considering the oscillator strengths of the different allowed transitions in a pump−probe experiment on homo- and heterodimers with strong coupling (see Figure 8) and then by taking into account how these oscillator strengths influence the pump−probe signal at different delay times.

The one- and two-exciton-state energies and related transition dipole strengths have been calculated using the structural model and parameters of the exciton Hamiltonian determined in ref 24 (for basic equations, see refs 31 and 32). The transitions from the ground to the one-exciton states are observed in the linear spectra depicted in Figure 7. We note that there is a slight 1−2 nm red shift of the bleachings in Figure 7 with respect to the wavelengths reported in Figure 9, which is due to the exciton−vibrational coupling that was included in the line shape theory of the spectra in Figure 7.

In order to interpret the pump−probe spectra we first decided which of the exciton levels was populated at a given delay time and then used the oscillator strengths and transition energies in Figure 8 to estimate the contribution of excited-state absorption

(ESA), stimulated emission (SE), and ground-state bleaching (GB). On the basis of the exciton relaxation calculations described in ref 24 we expect for homodimers exciton relaxation times < 100 fs, whereas for the heterodimers a relaxation time of 450 fs is obtained. On the basis of the assumption that internal conversion from the Soret bands into the exciton states of the dimers is markedly faster than 450 fs, the high-energy exciton state of the heterodimers is significantly populated. On the other hand, the excitons will already completely relax to the low-energy exciton states in the homodimers at delay times of 300 fs.

In the upper panels of Figure 9 the expected stick spectra are compared with the experimental data at 300 fs (taken from Figure 5), assuming that at short delay times the low-energy exciton state of the homodimers and the high-energy exciton state of the heterodimers are populated. The main bleaching at 660 nm is caused by the composite of GB and SE of the high-energy exciton state in the heterodimer, whereas the bleaching at 675 nm is determined by the GB of the high-energy exciton state in the homodimer. The small GB/SE of the low-energy exciton state of the homodimer occurs at 680 nm. There is a noticeable ESA at 678 nm in the calculated stick spectra that is found only at longer wavelength (695 nm) in the experiment. The origin of this discrepancy might be caused by neglecting the two-exciton shift, which can be caused by the charge density coupling between the pigments. In the calculation of the stick spectra a homo- to heterodimer ratio of 1 is assumed in the case of $x = 4.2$ that results in a ratio of one-half in the case of $x = 2.6$. The lower number of homodimers explains why for small x the bleaching at 675 nm is smaller than that for $x = 4.2$.

In the lower part of Figure 9 the stick spectra and experimental data are compared for delay times of ≥1 ps, assuming that in this case the excitons in the heterodimers are relaxed to the low-energy exciton state also. The ESA at 660 nm in the heterodimers cannot fully compensate the GB, an effect of the excitonic coupling, and therefore, even at long delay times a negative signal is detected in the pump−probe spectrum at 660 nm. The difference in the spectral position of the low-energy bleaching (at 675−680 nm) for different values of Chl *a*:Chl *b* ratios x is caused by the difference in relative contribution of GB of homodimers (674 nm) and GB/SE of heterodimers (678 nm).

The considerations within the framework of the exciton model[24] offer a qualitative picture of the exciton relaxation in the heterodimers and how it is reflected in the measured time-resolved transient absorption spectra. However, one puzzling point remains to be discussed: the calculated exciton relaxation time constant of 450 fs[24] is in very close correspondence with the experimentally obtained value of 400 fs, but the experimental spectra at delay times of 1 ps clearly show a stronger bleaching at 660 nm than the stick spectra where exciton relaxation in the heterodimers should be completed. One possible explanation for both the additional relaxation times and the additional GB is the presence of additional heterodimers with weak excitonic coupling, where the Chl *b* absorbs around 660 nm and Chl *a* around 675 nm. An alternative possibility would be a significantly different exciton−vibrational coupling in some dimers so that the exciton relaxation is slowed down, in spite of similar excitonic coupling strength. However, the large decrease in relaxation rates from $(400\ \text{fs})^{-1}$ to $(7-8\ \text{ps})^{-1}$ could only be explained by a drastic reduction of the Huang Rhys factor and/or a large increase of the correlation radius of the protein, which describes how well the modulation of different site energies

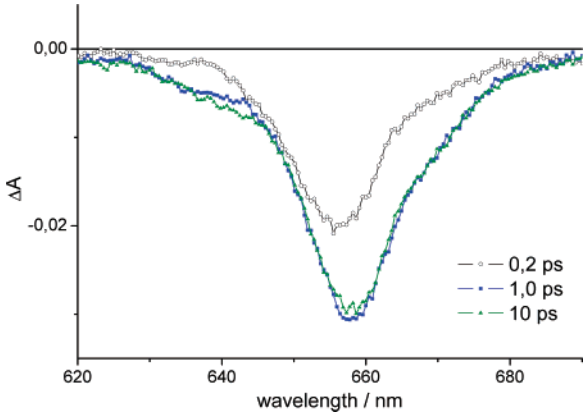

Figure 10. Transient absorption difference spectra of WSCP containing exclusively Chl *b*. Excitation wavelength: 640 nm ($\tau \approx 70$ fs, $E = 180$ nJ).

are correlated. A Huang Rhys factor of 0.8 was estimated from the temperature dependence of the linear absorption of the Chl *b* homodimers and the correlation radius of 5 Å from calculations of transient absorption data on a different system (for a detailed discussion, see ref 24). These values explain the fast component of the exciton relaxation. However, it is not very likely that the pigment−protein coupling varies to an extent that is required to account for 7−8 ps relaxation times. For example, an increase of the correlation radius by a factor of 2 requires a concomitant decrease of the Huang Rhys factor down to 12.5% of its original value. Such small Huang Rhys factors of 0.1 are unusual for pigment−protein complexes and would also not explain the temperature dependence of the absorption spectrum. Hole burning experiments (ref 33) could provide an independent estimation of the Huang−Rhys factor, and two-color photon echo experiments were shown recently to provide information on the correlation of the exciton−vibrational coupling at different sites (ref 34).

The spectral properties of the WSCP samples containing exclusively Chl *b* revealed the existence of two different energy levels in the Q_y region at about 655 and 665 nm, originating from excitonic splitting as a result of strong pigment−pigment coupling.[24] In order to unravel the excited singlet-state dynamics in these complexes the samples were excited at different wavelengths in the 640−660 nm range. For direct excitations into the high-energy exciton state at 655 nm, no change in the pump−probe signal could be detected for the delay times that can be achieved with the present time resolution of 200 fs. This finding is in perfect agreement with our calculations for exciton relaxation times between the high- and low-energy exciton states, which are in the range of <100 fs in the homodimers.[24] The exciton theory predicts a strong ESA at short wavelengths during population of the high-energy exciton state similar to that of the Chl a homodimer. Detection of this ESA will be an important signature of the population of the high-energy exciton state of the homodimer. This effect remains to be studied in future experiments of transients at higher time resolution.

Interestingly, at an excitation wavelength of 640 nm in the "blue edge" of the absorption profile of the Q_y band some dynamics are observed between 200 fs and 1 ps as shown in Figure 10.

Immediately after excitation the bleaching of the sample exhibits its peak position at around 654 nm. This peak shifts with increasing delay times toward longer wavelengths and reaches a value of 657.5 nm at 500 fs. No further changes of the bleaching can be recognized in the range of up to 10 ps

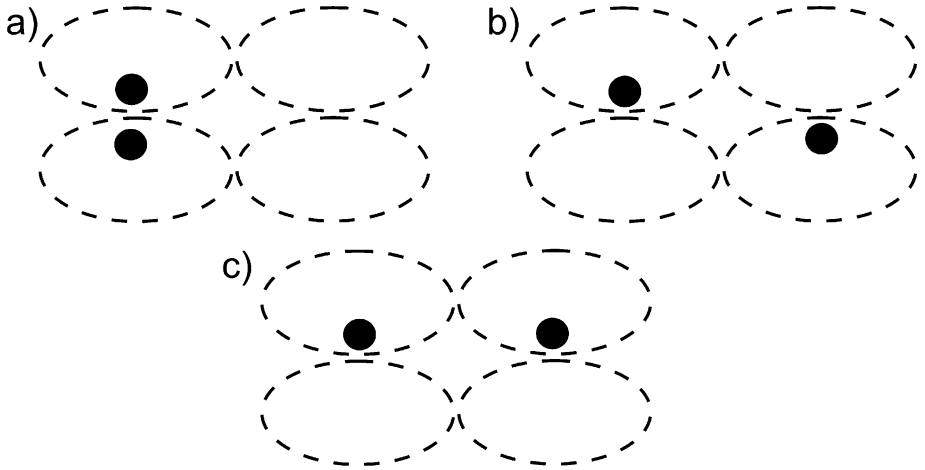

Figure 11. Possible arrangement of two pigments in the WSCP tetramer: (a) face-to-face attachment of two adjacent subunits, (b) "diagonal", and (c) "adjacent weakly coupled" array of two chlorophyll-containing WSCP subunits. The orientation of the pigments can be considered to be analogous to Horigome et al.[25]

delay time. These dynamics are likely not a reflection of exciton relaxation in strongly coupled homodimers (see above). As in the case of heterodimers, hole-burning experiments would offer a tool to observe the lifetime broadening of the exciton states.

Discussion

The present measurements of the ground-state absorption and CD spectra and their numerical evaluation[24] confirm the binding of two Chl molecules to the recombinant WSCP from cauliflower, thus forming a tetrameric complex. Results obtained on WSCP samples with greatly varying total Chl concentration in the reconstitution assay lead to the conclusion that the arrangement of two Chls within the WSCP tetramer is the dominant structure, i.e., the existence of complexes containing one, three, or four Chls per tetramer is of low probability.

As a consequence of these findings the binding of the two Chls appears to be a highly cooperative process that simultaneously prevents occupation of the potential binding sites in the two remaining subunits of the tetramer. This feature can be explained by the assumption that two WSCP units, each containing a single bound Chl, dimerize under the concomitant association with two further apoproteins to build the tetramer. Accordingly, this formation of the tetrameric complex would imply a "closure" of the remaining two sites for further pigment binding. This idea is in line with former results showing that saturation binding of Chls leads to WSCP complexes with a stoichiometry of two Chls/tetramer.[10] On the other hand, it is likely that WSCP samples reconstituted at a very low Chl concentration contain a minor population with only one Chl in complexes that are probably not oligomerized to tetramers. However, formation of a tetramer with a single Chl cannot be ruled out because this type of complex has been reported for a WSCP from Brussels sprouts.[21] At present no experimental data are available on the pathway of Chl binding and tetramer formation of the WSCP neither for in vivo assembly in the plant cell nor under in vitro reconstitution condition.

Now questions arise on the mode of binding of the two Chls within the WSCP tetramer. It was recently proposed by Krausz and co-workers[23] that the binding of two Chl a molecules leads to formation of an "open sandwich"-type pigment dimer with strong excitonic coupling. On the basis of an analysis of low-temperature (1.7 K) absorption, circular dichroism (CD), and magnetic circular dichroism (MCD) spectra within the framework of a simple exciton theory, Hughes et al.[23] obtained values of 60° and 7.6 Å for the tilt angle and the center-to-center (Mg−Mg) distance, respectively, of the two chlorin rings. A slightly larger angle of 70° was reported for the Chl *d* dimer.[23]

The proposal of an "open sandwich" was adopted for a thorough theoretical analysis of our spectral data. It was shown[24] that a consistent description can be achieved for both Chl *b*−Chl *b* homodimers and Chl *a*−Chl *b* heterodimers if the tilt angle is diminished to about 30°. Likewise, a reevaluation of the experimental data of Hughes et al.[23] revealed that use of the same tilt angle of 30° also permits a description of the optical properties of the Chl *a*−Chl *a* homodimer if the use of Gaussian bands gathered from the spectral deconvolution are replaced by spectra based on calculations with a microscopic theory, thus taking into account lifetime broadening of exciton transitions (for details see, ref 24). Therefore, it seems reasonable to assume that all strongly coupled Chl dimers formed in the recombinant WSCP tetramer are arranged as "open sandwiches" with an angle of about 30° regardless of the different substituents at the porphyrin rings in Chl *a*, Chl *b*, and Chl *d*. This conclusion can be even more generalized based on the first report on the X-ray crystal structure (at 2.0 Å resolution) of a WSCP isolated from *Lepidium virginicum* (Virginia pepperweed)[25] that was just published after completion of the present study. As this WSCP belongs to Class IIB—in contrast to the WSCP used in this study, which is a member of Class IIA—the new findings strongly support the idea that the "open sandwich" motif of Chl binding is characteristic for WSCPs. As a consequence, it appears attractive to consider possible functional implications of the geometry. This problem however is beyond the scope of the present study and remains to be clarified in further investigations.

Complementary information on the properties of the Chl dimers in the WSCP tetramers can be gathered from the results of time-resolved flash-induced absorption changes. The decay and rise in the bleaching of Chl *b* of Chl *a*, respectively, are both characterized by biphasic kinetics with typical time constants of 400 fs and 7−8 ps. This striking biphasic behavior suggests that the sample is heterogeneous. The 400 fs kinetics can be consistently explained by relaxation within the strongly coupled Chl *a*−Chl *b* heterodimer from the upper exciton state with its dominant "Chl *b* character" to the lower one of mainly "Chl *a* character".[24] On the other hand, the slower component of 7−8 ps is unlikely to reflect a strongly retarded transition from the upper to the lower exciton level. It seems more

reasonable to assume the existence of Chl *a*−Chl *b* dimers that are weakly coupled due to a larger separation of the Chl moieties. An attractive idea to rationalize the putative sample heterogeneity could be the assumption that several types of dimers with different pigment array exist in the tetrameric protein matrix as illustrated in Figure 11: (i) "open sandwich" configuration formed by face-to-face attachment of two subunits with a bound Chl molecule and "side-on" binding of the other two subunits with empty binding sites (a) and (ii) attachment of two Chl-containing subunits that prevents exciton coupling by either a diagonal (b) or an "adjacent weakly coupled" (c) array of the two WSCP subunits each containing one Chl and complementary array of the two other subunits with an empty binding site. In these two types of Chl *a*−Chl *b* heterodimers (b and c) the excitation energy transfer from Chl *b* to Chl *a* occurs via a Förster-type process. At present, however, no direct experimental evidence exists for this model of sample heterogeneity.

Formation of a strongly coupled Chl dimer in WSCP is surprising because excitonic coupling is typical for all reaction centers and photosystems where a "special pair"-type dimer motif exists within the array of the pigment cofactors that are involved in light-induced charge separation.[35] In anoxygenic photosynthetic bacteria a special pair P of two bacteriochlorophylls (BChl) acts as the primary electron donor for formation of the radical pair $P^{+\bullet}$ $Bpheo^{-\bullet}$ (for a review, see ref 36), while in the photosystems the "dimeric" motif of Chl *a*−Chl *a*′ in PS I[37] and of Chl *a*−Chl *a* (P_{D1}−P_{D2}) in PS II[38] most likely function as secondary electron donors to a photoactive monomeric Chl that forms the primary cation radical by electron ejection from its lowest excited singlet state and transfer to the primary acceptors (for discussions, see refs 35 and 39). Inspection of the structures of these "special pairs" (for recent reviews of purple bacteria, PS I, and PS II, see Lancaster,[40] Fromme et al.,[41] and Zouni,[42] respectively) readily shows that the pigment arrangement of the putative "open sandwich" dimer in WSCP is entirely different. The different geometry of the excitonically coupled pigments in both types of dimers also leads to a marked contrast in the oscillator strength distribution between the two exciton states. In all "special pairs" the lower exciton state carries most of the oscillator strength, while the opposite was shown to be the case in the WSCP (vide supra). A similar feature of excitonic coupling as in reaction centers is also observed in antenna systems, e.g., in LH 2 of anoxigenic bacteria where B850 represents a strongly absorbing lower exciton band of the strongly coupled BChls. This drastically different feature is not surprising when considering the different functions of reaction centers/photosystems and antenna systems versus the possible functions of WSCP. Questions rather arise on possible functional reasons for formation of this type of strongly coupled dimers of chlorophyll in WSCP. The trivial case of the "open sandwich" dimer being a unique binding motif of the in vitro system that does not reflect the structure of the native cauliflower WSCP can be ignored because the reconstituted samples exhibit absorption and fluorescence spectra that are identical to those of purified WSCP isolated from cauliflower.[11] This finding strongly supports the idea that the "open sandwich" dimer is also formed in vivo in class IIA WSCPs (for a review on WSCP types, see Satoh et al.[10]). The new crystal structure data reveal that this structural motif also exists in Class IIB WSCP.[25] If one considers the proposed function of the WSCP as a transport protein of Chl (and related compounds) it seems attractive to speculate on a protective dimer that avoids dissipative side reactions due to singlet oxygen formation. Unfortunately, this mode of action can also be ruled out on the basis of the results of fluorescence lifetime measurements (Schmitt et al., manuscript in preparation). Therefore, the drastically reduced probability of $^1\Delta_gO_2$ formation in WSCP[16] most likely originates from a barrier to the direct interaction between O_2 and Chl that is established by the proteins, as also proposed by Horigome et al.[25] for the class IIB WSCP from *Lepidium virginicum*. The sensitized reaction of ^{3}Chl with ground-state $^3\Sigma_gO_2$ requires the contact between the reactants.[43]

At present we cannot offer a convincing explanation for a possible physiological role of this particular mode of Chl binding in the WSCP, but this study clearly shows the potential of WSCP in offering a most suitable material for analyzing fundamental aspects of Chl−Chl and Chl−protein interactions in natural Chl−protein complexes.

References and Notes

(1) Renger, G. In *Primary Processes of Photosynthesis: Basic Priniciples and Apparatus*; Renger G., Ed.; Royal Society of Chemistry: Cambridge 2007; Vol. I, p 7.

(2) Green, B. R.; Anderson, J. M.; Parson, W. W. In *Light harvesting antennas in Photosynthesis*; Green, B. R., Parson, W. W., Eds.; Kluwer: Leiden, 2003.

(3) Renger, G. In *The Photosystems: Structure, Function and Molecular Biology*; Barber, J., Ed.; Elsevier: Amsterdam, 1992; p 45.

(4) van Grondelle, R.; Dekker, J. P.; Gillbro, T.; Sundstrom, V. *Biochim. Biophys. Acta* **1994**, *1187*, 1.

(5) Krupa, Z.; Williams, J. P.; Mobashoher, Khan U.; Huner, N. P. A. *Plant Physiol.* **1992**, *100*, 931.

(6) Nussberger, S.; Dörr, K.; Wang, D. N.; Kühlbrandt, W. *J. Mol. Biol.* **1993**, *234*, 347.

(7) Paulsen, H. *Photochem. Photobiol.* **1995**, *62*, 367.

(8) Morosinotto, T.; Bassi, R. In *Primary Processes of Photosynthesis: Basic Priniciples and Apparatus*; Renger, G., Ed.; Royal Society of Chemistry: Cambridge, in press; Vol. I.

(9) van Amerongen, H.; Croce, R. In *Primary processes of photosynthesis: Basic principles and Apparatus*; Renger, G., Ed.; Vol. I, Royal Society of Chemistry: Cambridge, in press; Vol. I.

(10) Satoh, H.; Uchida, A.; Nakayama, K.; Okada, M. *Plant Cell Physiol.* **2001**, *42*, 906.

(11) Satoh, H.; Nakayama, K.; Okada, M. *J. Biol. Chem.* **1998**, *273*, 30568.

(12) Downing, W. L.; Mauxion, F.; Fauvarque, M.-O.; Reviron, M.-P.; de Vienne, D.; Vartanian, N.; Giraudat, J. *Plant J.* **1992**, *2*, 685.

(13) Reviron, M.-P.; Vartanian, N.; Sallantin, M.; Huet, J.-C.; Pernollet, J.-C.; de Vienne, D. *Plant Physiol.* **1992**, *100*, 1486.

(14) Annamalai, P.; Yanagihara, S. J. *Plant Physiol.* **1999**, *155*, 226.

(15) Nishio, N.; Satoh, H. *Plant. Physiol.* **1997**, *115*, 841.

(16) Schmidt, K.; Fufezan, C.; Krieger-Liszkay, A.; Satoh, H.; Paulsen, H. *Biochemistry* **2003**, *42*, 7427.

(17) Matile, P.; Schellenberg, M.; Vicentini, F. *Planta* **1997**, *201*, 96.

(18) Kräutler, B.; Hörtensteiner, S. In *Chlorophylls and Bacteriochlorophylls, Advances in Photosynthesis and Respiration*; Grimm, B., Porra, R. J., Rüdiger, W.; Scheer, H., Eds.; Springer: Heidelberg, 2006; Vol. 25, p 237.

(19) Schmid, H. C.; Oster, U.; Kögel, J.; Lenz, S.; Rüdiger, W. *Biol. Chem.* **2001**, *382*, 903.

(20) Reinbothe, C.; Satoh, H.; Alcaraz, J.-P.; Reinbothe, S. *Plant Physiol.* **2004**, *134*, 1355.

(21) Kamimura, Y.; Mori, T.; Yamasaki, T.; Katoh, S. *Plant Cell Physiol.* **1997**, *38*−*2*, 133.

(22) Green, B. R.; Durnford, D. G. *Annu. Rev. Plant Physiol. Plant Mol. Biol.* **1996**, *47*, 685.

(23) Hughes, J. L.; Razeghifard, R.; Logue, M.; Oakley, A.; Wydrzynski, T.; Krausz, E. *J. Am. Chem. Soc.* **2006**, *128*, 3649.

(24) Renger, T.; Trostmann, I.; Theiss, C.; Madjet, M. E.; Richter, M.; Paulsen, H.; Eichler, H. J.; Knorr, A.; Renger, G. *J. Phys. Chem. B* **2007**, *111*, 10487.

(25) Horigome, D.; Satoh, H.; Itoh, N.; Mitsunaga, K.; Oonishi, I.; Nakagawa, A. *J. Biol. Chem.* **2007**, *282*, 6525.

(26) Paulsen, H.; Rümler, U.; Rüdiger, W. *Planta* **1990**, *181*, 204.

(27) Hobe, S.; Fey, H.; Rogl, H.; Paulsen, H. *Biol. Chem.* **2003**, *278*, 5912.

(28) O'Shea, P.; Kimmel, M.; Gu, X.; Trebino, R. *Opt. Lett.* **2001**, *26*−*12*, 932.

(29) Murata, T.; Toda, F.; Uchino, K.; Yakushiji, E. *Biochim. Biophys. Acta* **1971**, *245*, 208.

(30) Scheer H. In *Chlorophylls and Bacteriochlorophylls*; Grimm, B., Porra, R. J., Rüdiger, W., Scheer, H., Eds.; Springer: Heidelberg, 2006; p 1.

(31) Van Amerongen, H.; Valkunas, L.; van Grondelle, R. *Photosynthetic Excitons*; World Scientific: Singapore, 2000; pp 89−94.

(32) Renger, T.; Voigt, J.; May, V.; Kühn, O. *J. Phys. Chem.* **1996**, *100*, 15654.

(33) Melkozernov, A. N.; Blankenship, R. E. *Photosynth. Res*. **2005**, *85*, 33.

(34) Lee, H.; Cheng, Y.-C.; Fleming, G. R. *Science* **2007**, *316*, 1462.

(35) Renger, G.; Holzwarth, A. R. In *Photosystem II: The Light-Driven Water:Plastoquinone Oxidoreductase*; Wydrzynski, T., Satoh, K., Eds.; Springer: Heidelberg, 2005; p 139.

(36) Parson, W. W. In *Photosynthesis*; Amesz, J., Ed.; Elsevier: Amsterdam, 1987; p 43.

(37) Jordan, P.; Fromme, P.; Witt, H. T.; Klukas, O.; Saenger, W.; Krau, N. *Nature* **2001**, *411*, 909.

(38) Loll, B.; Kern, J.; Saenger, W.; Zouni, A.; Biesiadka, J. *Nature* **2005**, *438*, 1040.

(39) Holzwarth, A. R.; Müller, M. G.; Niklas, J.; Lubitz, W. *Biophys. J.* **2006**, *90*, 552.

(40) Lancaster, R. In *Primary Processes of Photosynthesis: Basic Principles and Apparatus*; Renger, G., Ed.; Royal Society of Chemistry: Cambridge, 2007; Vol. II, p 5.

(41) Fromme, R.; Grotjohann, I.; Fromme, P. In *Primary Processes of Photosynthesis: Basic Principles and Apparatus*; Renger, G., Ed.; Royal Society of Chemistry: Cambridge, 2007; Vol. II, p 110.

(42) Zouni, A. In *Primary Processes of Photosynthesis: Basic Principles and Apparatus*; Renger, G., Ed.; Royal Society of Chemistry: Cambridge, 2007; Vol. II, p 193.

(43) Drzewiecka-Matuszek, A.; Skalna, A.; Karocki, A.; Stochel, G.; Fiedor, L. *J. Biol. Inorg. Chem.* **2005**, *10*−*5*, 453.

(44) Halls, C. E.; Rogers, S. W.; Oufattole, M.; Østergard, O.; Svensson, B.; Rogers, J. C. *Plant Sci.* **2006**, *170*, 1102.